



The National Center for Hypersonic  
Laminar-Turbulent Transition Research

# Surface Roughness Effects on a Blunt Hypersonic Cone

Nicole Sharp  
Jerrod Hofferth  
Edward White

Texas A&M University  
November 2012



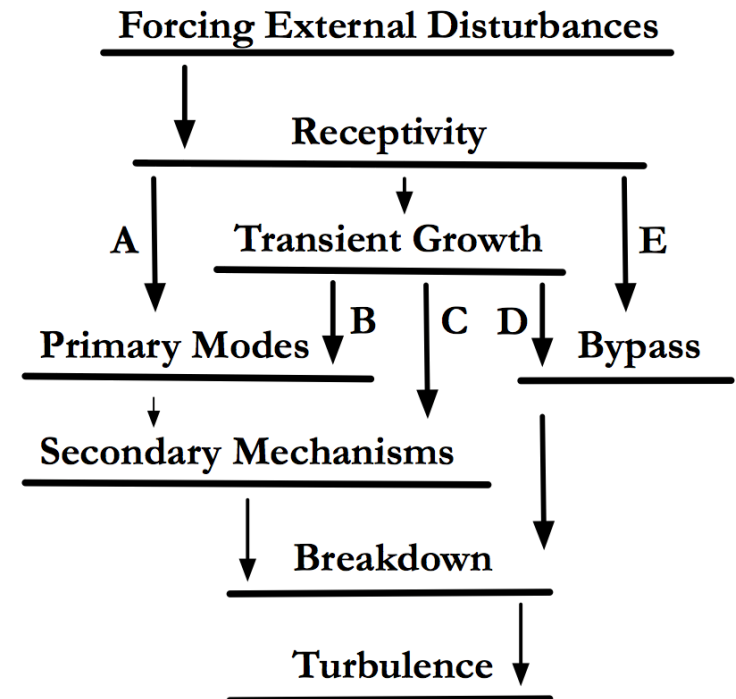


- Real hypersonic surfaces are rough.
- Isolated roughness includes:
  - Fasteners
  - Joints
  - Tripping elements
  - Gap filler
- Distributed roughness
  - Machining marks
  - Ablative heat shields
  - Thermal protection tiles



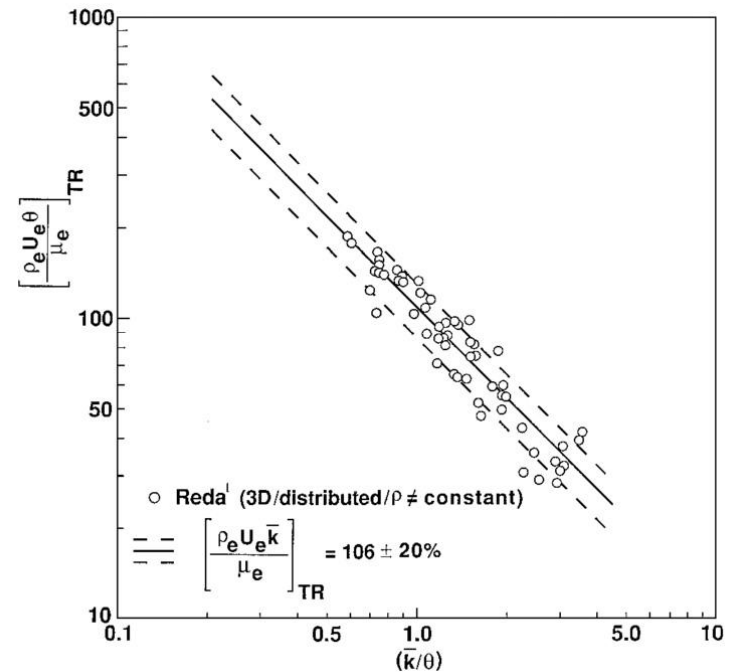


- Surface roughness introduces disturbances into the boundary layer, which may be enhanced through transient growth.
- Transient growth, being nonmodal in nature, can exist in regions subcritical to other transition mechanisms.
- The “blunt-body paradox,” in which transition occurs earlier than predicted even on highly polished surfaces, may be explicable through roughness-induced transient growth.





- Computations of surface roughness are expensive, except in cases of isolated roughness.
- Existing literature on experimental roughness-induced transition is vast, but:
  - Focuses on empirical correlations for transition prediction
  - Often utilizes noisy, conventional wind tunnels
- Physics-based transition correlation is desirable.

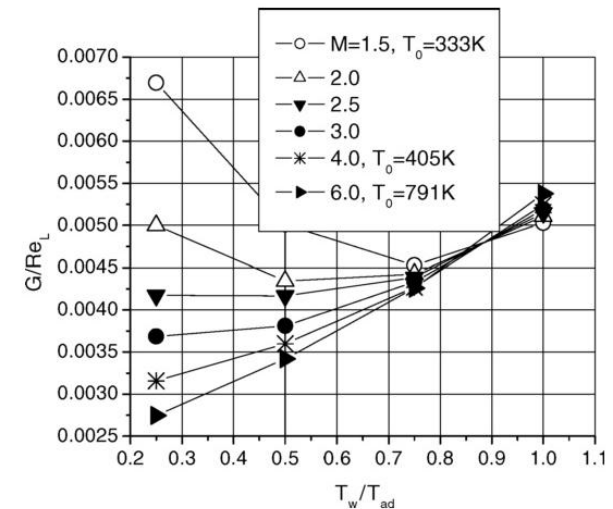


Nosetip transition data from ballistics-range experiments; three-dimensional distributed roughness, compressible flows (Reda 2002).

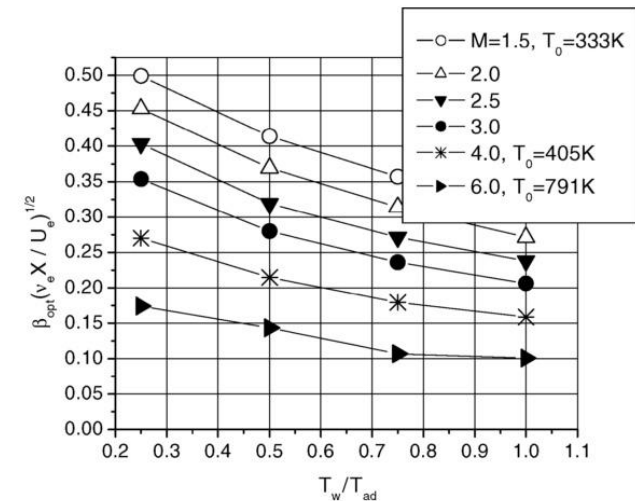




- Computations of optimal disturbances for compressible boundary layers exist:
  - Flat plate/cone, sphere (parallel): Reshotko and Tumin (2004)
  - Flat plate, sphere (non-parallel): Zuccher *et al* (2006)
  - Sharp cone (non-parallel): Zuccher *et al* (2007)
- Transient growth is destabilized by wall cooling and increasing spherical radius but stabilized by flow divergence.
- Low-speed experiments indicate roughness induces suboptimal disturbance growth (White 2002, White *et al* 2005).



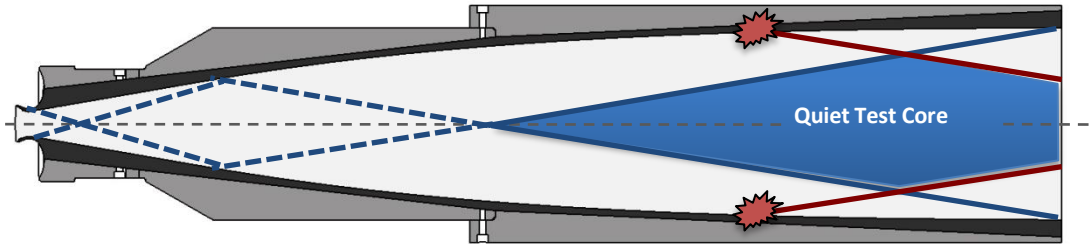
Optimal growth factors for zero pressure gradient;  $Re_L = 9 \times 10^4$  (Reshotko and Tumin 2004).



Optimal spanwise wavenumber for zero pressure gradient;  $Re_L = 9 \times 10^4$  (Reshotko and Tumin 2004).



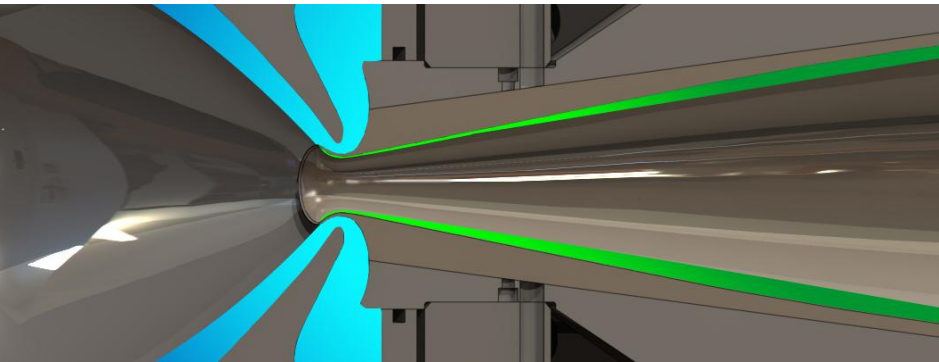
# Mach 6 Quiet Tunnel (M6QT)



Straight-wall section and slow expansion contour minimizes growth of the Görtler instability

Quiet test core defined upstream by Mach 5.91 uniform flow and downstream by acoustic disturbances generated by nozzle-wall turbulent boundary-layer eddies and radiated along Mach waves

- Low-disturbance test environment up to a  $Re = 10 \times 10^6 \text{ m}^{-1}$
- 40 second nominal run-time
- Hotwire anemometry used as primary diagnostic (presently uncalibrated)

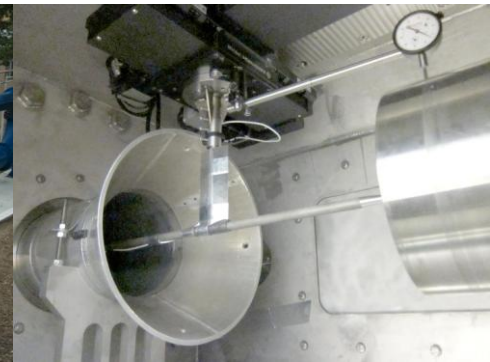


Settling chamber boundary layer removed via vacuum ejectors, initiating new laminar boundary layer on nozzle

Toggleing bleed valves allows quiet ( $0.05\% \text{ Pt}'/\text{Pt}$ ) or noisy operating conditions



Vacuum-pressure blow-down configuration using a two-stage air ejector system



Enclosed free-jet test section with two-axis traverse



# Smooth, 5-degree cone with interchangeable nosetips



1.59 mm radius, smooth



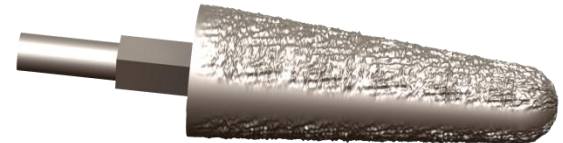
1.59 mm radius, discrete roughness elements



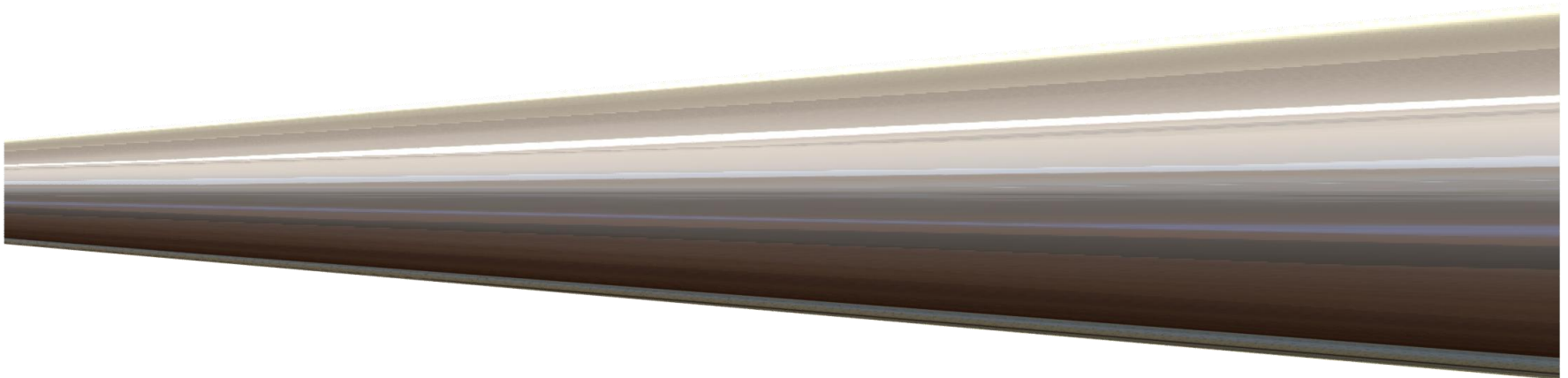
6.35 mm radius, smooth



6.35 mm radius, discrete roughness elements



6.35 mm radius, quasi-random distributed roughness





# Quasi-random distributed roughness



6.35 mm radius nosetips, quasi-randomly distributed roughness (left) and nominally smooth (right)

- Roughness generated via Fourier series

$$h(x, \theta) = \sum_{n=1}^N \sum_{m=1}^M A_{n,m} \cos\left(\left(2\pi n x / \lambda_k \cos \gamma_c\right) + m K \theta + \phi_{n,m}\right)$$

$x$  = axial coordinate

$\theta$  = azimuthal angle

$\gamma_c$  = half-angle =  $5^\circ$

$\phi_{n,m} \in U(0, 2\pi)$

$K = 12$ , for  $30^\circ$  periodicity

$N = M = 5$

$\lambda_k = 10.16$  mm

$Max(A_{n,m}) = 0.635$  mm

- Roughness repeats over two  $150^\circ$  arcs separated by two  $30^\circ$  sections of nominally smooth surface
- $A_{n,m}$  coefficients selected from a half-normal distribution and scaled

- Quasi-random distributed roughness nosetip constructed via direct metal laser sintering





## Initial experiments

- Tested 6.35 mm radius smooth and distributed rough nosetips



6.35 mm radius nosetips, quasi-randomly distributed roughness (left) and nominally smooth (right)

Table 1: Experimental conditions			
Parameter	Condition 1	Condition 2	Condition 3
Nominal $M$	5.9	5.9	5.9
$P_o$	551 kPa	689 kPa	896 kPa
$T_o$	430 K	430 K	430 K
$Re$	$6.1 \times 10^6 \text{ m}^{-1}$	$7.7 \times 10^6 \text{ m}^{-1}$	$10 \times 10^6 \text{ m}^{-1}$
$Re_n$	$3.9 \times 10^4$	$4.9 \times 10^4$	$6.3 \times 10^4$

$$Re_{\theta} \left( \frac{k}{\theta} \right) = \frac{U_e k}{\nu_e}$$

Transition predicted by Reshotko (2007) above ~250-300 (flat plate).

- For  $k = 0.11 \text{ mm}$ :

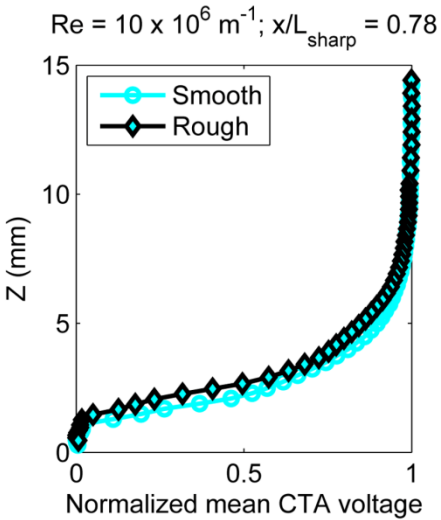
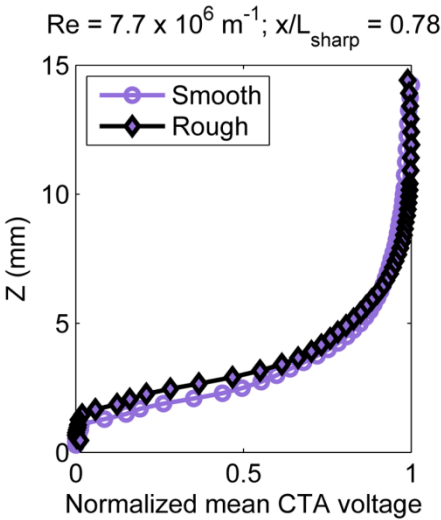
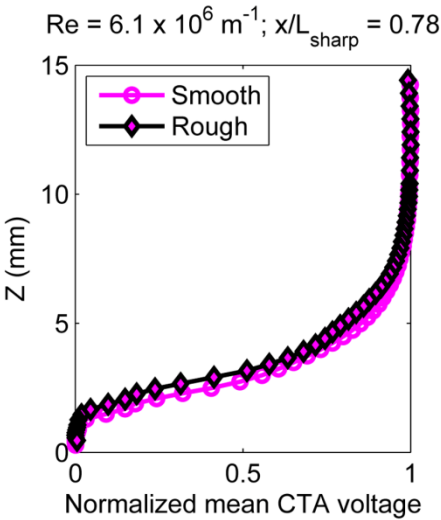
$$\frac{U_e k}{\nu_e} = 780 \text{ to } 1340$$

- Wall-temperature during run is 5-8% higher than adiabatic due to subsonic preheating.

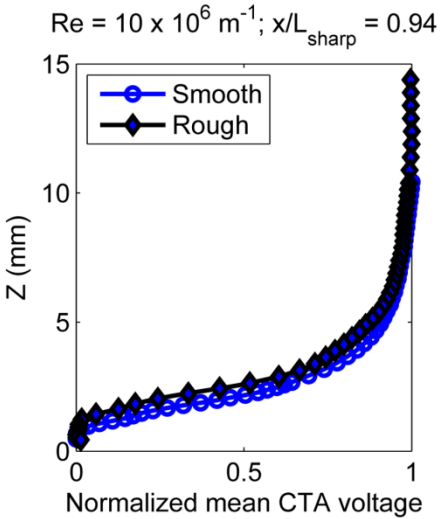
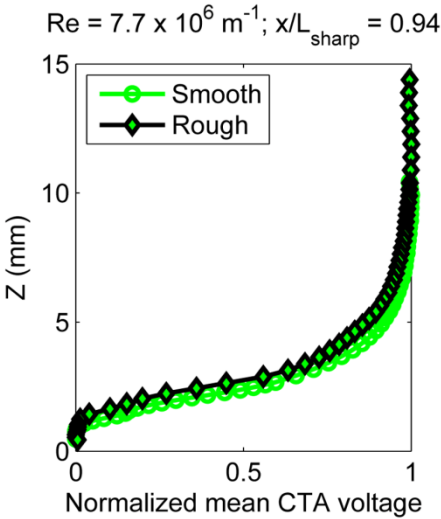
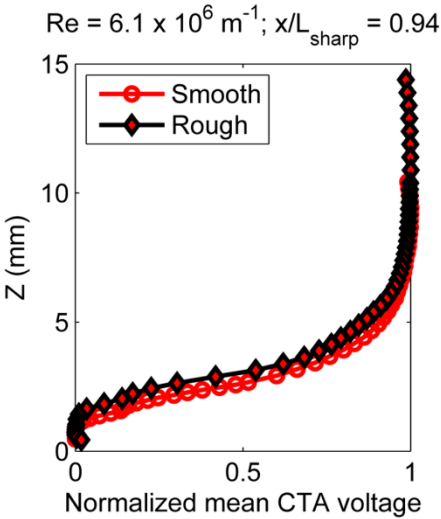


# Mean boundary layer profiles

Increasing streamwise distance  
↓



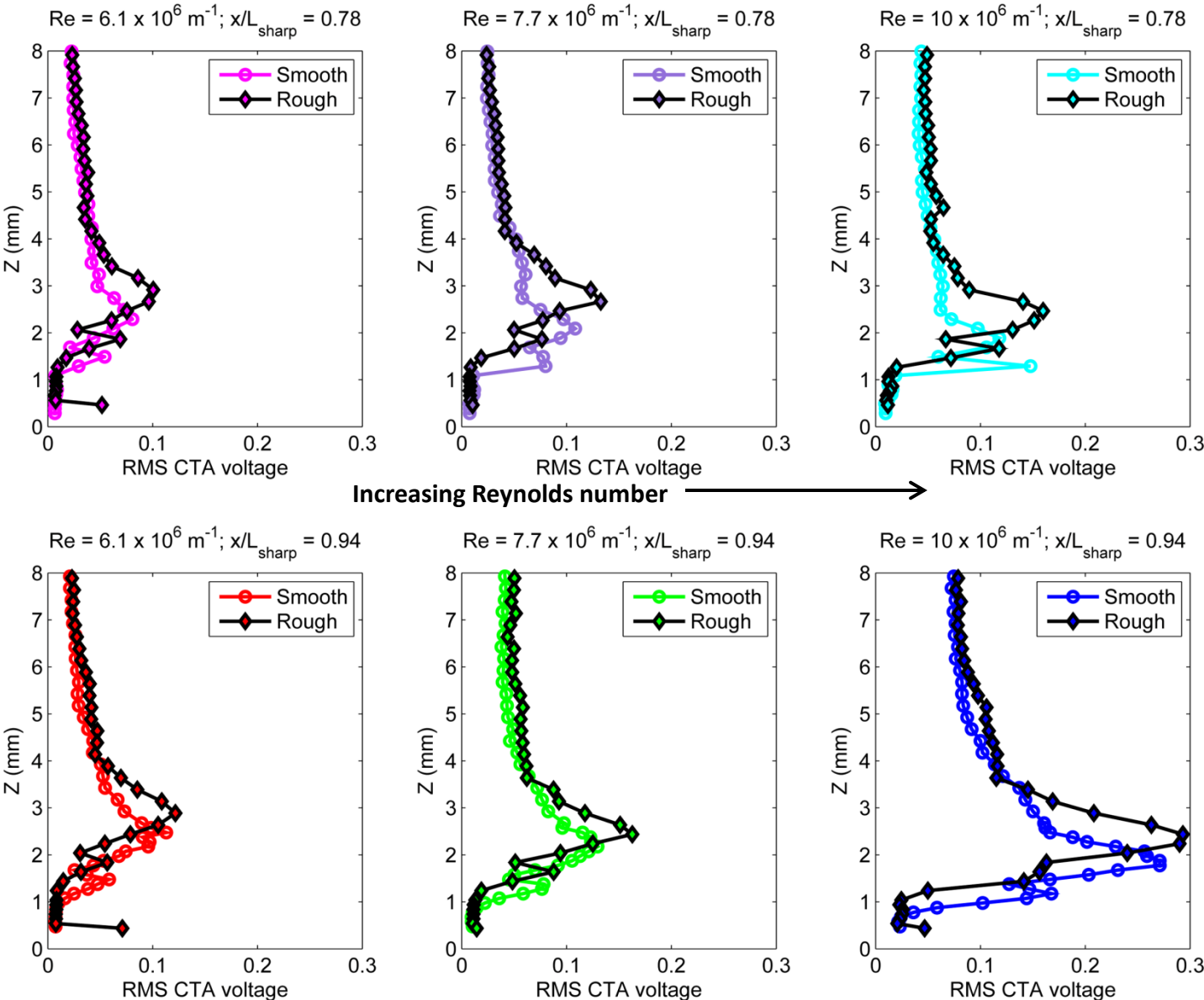
Increasing Reynolds number →





# RMS fluctuation profiles

Increasing streamwise distance  
↓





# Conclusions



- Growth of fluctuation amplitudes is observed but distributed roughness only marginally increases growth compared to a smooth wall.
- The distributed roughness nosetip is insufficient to trip the boundary layer, possibly due to the bluntness of the nose.
- Future experiments will include:
  - azimuthal measurements for detection of streaky structures to confirm transient growth
  - sharper nosetips and discrete roughness elements spaced according to optimal disturbance theory

# Acknowledgements

